JOINT CONFERENCE PROCEEDINGS
9th International Conference on Urban Earthquake Engineering/ 4th Asia Conference on Earthquake Engineering
March 6-8, 2012, Tokyo Institute of Technology, Tokyo, Japan

ELASTIC AND POST-ELASTIC RESPONSE OF STRUCTURES TO HYBRID BROADBAND SYNTHETIC GROUND MOTIONS

Carmine Galasso[1)], Farzin Zareian[2)], Iunio Iervolino[3)], and Robert W. Graves[4)]

1) Postdoctoral Fellow, Dept. of Civil and Environmental Engineering, University of California, Irvine, Irvine, CA, 92697, USA.
2) Assistant Professor, Dept. of Civil and Environmental Engineering, University of California, Irvine, Irvine, CA, 92697, USA.
3) Associate Professor, Dip. di Ingegneria Strutturale, Università degli Studi di Napoli Federico II, Naples, Italy.
4) Research Geophysicist, U.S. Geological Survey, Pasadena, CA, 91106, USA.
cgalasso@uci.edu, zareian@uci.edu, iunio.iervolino@unina.it, rwgraves@usgs.gov

Abstract: In this paper, a statistical comparison between seismic demands of single degree of freedom (SDOF) systems subjected to past events using simulations and actual recordings is provided. A number of SDOF systems are selected considering: (1) eighteen oscillation periods between 0.1s and 8s, (2) elastic case and four non-linearity levels, from mildly inelastic to severely inelastic structures, and (3) two hysteretic behaviors, namely non-degrading and non-evolutionary, and both degrading and evolutionary. Demand spectra in terms of peak and cyclic response and theirs statistics are derived for four historical earthquakes: 1979 M_w = 6.5 Imperial Valley, 1989 M_w = 6.8 Loma Prieta, 1992 M_w = 7.2 Landers, and 1994 M_w = 6.7 Northridge.
Results of this study show that both elastic and inelastic demands to simulated and recorded motions are generally similar. However, for some structural systems, the inelastic response to simulated accelerograms may produce demands that are different from that obtained using corresponding recorded motions. In the case of peak response, these discrepancies are due to differences in the spectral shape while the differences in terms of cyclic response can be explained by some integral parameters of ground motion (i.e., duration-related). Moreover, the intra-event standard deviation values of structural response calculated from the simulation are generally lower than those given by recorded ground motions. The amount of such differences strongly depends on the SDOF period and nonlinearity level, and to a lesser extent depends on the hysteretic model used. Assessment of the results using formal statistical hypothesis tests indicates that in most cases the differences are not statistically significant.

1. INTRODUCTION

The use of nonlinear dynamic analysis (NLDA) for assessment of existing structures, and design of new ones requires availability of reliable accelerograms. Usually, accelerograms are selected and scaled from a database of existing records to represent target seismic characteristics (e.g., hazard, magnitude, source-to-site distance, and local soil conditions). Numerous methods for such selection and scaling have been proposed. A summary of available ground motions (GMs) selection and scaling methods can be found in Haselton ed. (2009).

The inherent scarcity or total absence of suitable real (e.g., recorded during past earthquakes) GMs for some specific scenarios (e.g., recording of large magnitude strike-slip events with close site-source distances) makes utilization of alternative options unavoidable. This is the case, for example, for seismically active regions (such as California) where the spectral acceleration of interest is often relatively large and the hazard-controlling earthquake scenarios are often large magnitude events on nearby faults. Physics-based simulated (or synthetic) GMs capturing complex source features (such as spatially variable slip distributions, rise time, and rupture velocities), path effects (geometric spreading and crustal damping) and site effects (wave propagation through basins and shallow site response) provide a valuable supplement to recorded GMs, fulfilling a variety of engineering needs (Somerville, 1993). The general concern among engineers is that simulated records may not be equivalent to real records in estimating the seismic demand, and hence, the induced damages on structures (Naeim and Graves, 2005).

To validate synthetic GMs, some previous and concurrent studies have employed direct (i.e., by visual inspection) comparison of observed and simulated waveforms (especially in the case of low frequencies waveforms), or comparison in terms of median levels of observed and simulated intensity measures (including elastic spectral ordinates) for hybrid broadband simulation procedures (Olsen et al. 2003; Graves and Pitarka; 2010). Recently, Star et al. (2011) have compared elastic acceleration spectral ordinates (at several periods) from simulated motions for a M_w = 7.8 rupture scenario on the San Andreas Fault (two permutations with different hypocenter locations), and a M_w = 7.15 Puente Hills blind thrust scenario, to median and dispersion predictions from empirical *Next Generation Attenuation* (NGA) ground motion prediction equations (GMPEs). The identified discrepancies between results can indicate problems with the simulations, GMPEs, or perhaps both.

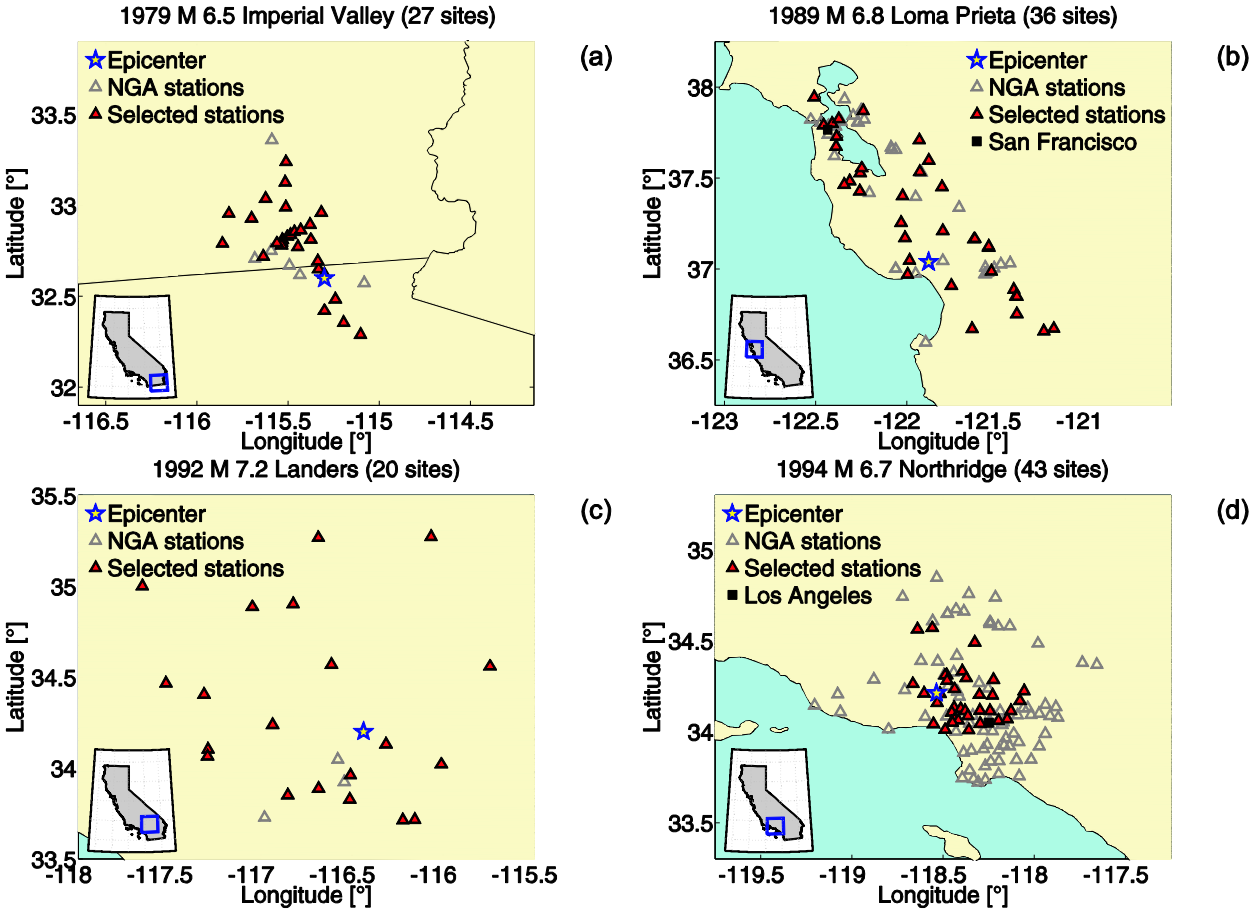

Figure 1 Maps of the considered earthquakes. The star is the epicenter and the grey triangles are recording stations of the NGA database for which the simulations are available. The red triangles are recording stations considered in this study. San Francisco (b) and Los Angeles (d) are also indicated on the map (black squares).

In this study we take a step back and try to understand if simulated GMs are comparable to real records in terms of their linear and nonlinear response in the single degree of freedom (SDOF) systems domain. Such investigation is a proxy for assessing the damage potential of simulated motions for many structural types. To this aim, Bazzurro et al. (2004a) addressed the issue of engineering validation in terms of elastic and inelastic SDOF structural response to seven suites of synthetic records that emulate real GMs recorded at 20 stations located within 20km from the Northridge fault rupture. The results show that six out of seven simulation methods appear to be biased, especially in the short period range, both in the linear elastic and in the nonlinear post-elastic regimes.

As post-elastic dynamic response of structures is of fundamental importance in performance-based earthquake engineering, the study presented in this paper focuses on the issue of engineering validation of GM simulation in terms of peak and cyclic demand of inelastic SDOF systems with different elastic and hysteretic characteristics. More specifically, two kinds of SDOF systems are considered by comparing their nonlinear response to simulated and recorded motions: (1) non-degrading and non-evolutionary, and (2) degrading and evolutionary. Demand spectra in terms of inelastic displacement and equivalent number of cycles are derived for different periods, strength factors and considering simulations for four historical Californian earthquakes. For each earthquake, we consider a real GM dataset, whose response statistics are used as a benchmark, and a synthetic GM dataset, including the same stations of the real dataset.

The aim here is to address, on a statistical basis, whether simulated GMs are systematically biased in terms of their median nonlinear response characteristics in comparison with real records. We also look into dispersion (i.e., intra-event variability) of response to recorded and simulated GMs. Hypothesis tests on selected samples are also carried out to assess the statistical significance of the results found in terms of both peak and cyclic response. In the end, the correlation between the SDOF seismic demands from simulated and recorded motions and duration and the presence of pulse-like records is investigated.

2. DESCRIPTION OF SYNTHETIC AND REAL GROUND MOTION DATASETS

Graves and Pitarka (2010) developed a hybrid broadband (0-10 Hz) GM simulation methodology which combines a physics-based deterministic approach at low

frequencies ($f \leq 1$ Hz, i.e. $T \geq 1$s) with a semistochastic approach at high frequency ($f > 1$ Hz, i.e., $T < 1$s). The low and high frequency waveforms are computed separately and then combined to produce a single time history. At frequencies below 1 Hz, the methodology contains a theoretically rigorous representation of fault rupture and wave propagation effects and attempts to reproduce recorded GM waveforms and amplitudes. At frequencies above 1 Hz, a stochastic representation of source radiation combined with a simplified theoretical representation of wave propagation and scattering effects are used to simulate waveforms. The use of different simulations approaches for the different frequency bands results from the seismological observation that source radiation and wave propagation effects tend to become stochastic at frequencies of about 1 Hz and higher, primarily reflecting the relative lack of knowledge about the details of these phenomena at higher frequencies. For both short and long periods, the effect of relatively shallow site condition, as represented by shear wave velocity in the upper 30 m (V_{s30}) are accounted for using the empirical site amplification model of Campbell and Bozorgnia (2008).

Four historical earthquakes recordings are modeled using the developed technique (Graves and Pitarka, 2010) and are used in the present study: 1979 M_w = 6.5 Imperial Valley, 1989 M_w = 6.8 Loma Prieta, 1992 M_w = 7.2 Landers, and 1994 M_w = 6.7 Northridge. In the simulation process, the required input parameters, related to the specific earthquake, are seismic moment, overall fault dimensions and geometry, hypocenter location and a generalized model of the final slip distribution; see also Graves and Aagaard (2011). For each earthquake event, the developed model covers a wide area surrounding the fault including several strong motion recording sites as in the NGA database: 33 for Imperial Valley, 71 for Loma Prieta, 23 for Landers and 133 for Northridge. These sites are shown with triangles in Figure 1.

A limited number of these sites are used in this study; only those with the real recordings' usable bandwidth larger than 0.1s-8s. This limitation yields a total of 126 sites for the entire study. These sites are marked with red triangles in Figure 1. Such large bandwidth for recorded motions provides justifiable means to cover a good range of nonlinear SDOF systems where period elongation can force the effective period of the system to be much larger than its initial period. In some cases, especially for degrading and evolutionary SDOF systems, as the damage severity progresses, the period elongation can force the SDOF period outside the suggested usable bounds, therefore, the usable lower frequency will tend to be somewhat higher (more restrictive). Moreover, the correlation between inelastic spectral ordinates at the fundamental period and at higher periods may be important. Hence, the results presented in this paper for very long period-structures (e.g., 6-8s), in the severely nonlinear range, should be considered with caution (see Bazzurro et al., 2004b for a discussion on this topic). However, the fact that, for some conditions, usable data are very sparse (or non-existent) and may affect the statistical significance of the findings of the study, it is also one of the principal situations under which simulations might be utilized.

3. DESCRIPTION OF THE SDOF SYSTEMS AND DEMAND MEASURES

The pool of GMs described in previous section, recorded and simulated, are used to perform NLDA on a total of 144 SDOF systems, representing combinations of variation in three parameters:

- SDOF fundamental period (T): periods between 0.1s and 8s are considered in this study. The period range is sampled with a 0.1s step from 0.1s to 0.5s, with a step of 0.25s between 0.5s and 1s, with a step of 0.5s between 1s and 5s, and with a step of 1s between 5s and 8s.
- Strength reduction factors (R): this parameter is the ratio of the GM record elastic demand and the yield strength of the SDOF system, F_y. R is varied in order to describe elastic/inelastic structural behavior; from elastic (R = 1), for completeness and checking purposes, to mildly inelastic (R = 2) and severely inelastic structures (R = 8). Note that the peak deformation experienced by an elastic structure is a GM and SDOF period specific quantity. We obtain F_y for a given R value for each record in the dataset (*constant-R approach*) to account for the large variability of the GM features (e.g., in terms of spectral ordinates), to follow. Then, each record is effectively applied to SDOF systems with slightly different strength characteristics. In contrast, in the *constant-strength* approach – not used in this study – a constant, "average" value of F_y (for example based on a given matched target spectrum) is used, for each period and R value, to assess the effect of different sets of accelerograms on the same structure.
- Hysteretic behavior: two hysteretic behaviors are considered in this study, i.e., non-degrading and non-evolutionary, and degrading and evolutionary. A non-degrading elastic-plastic with positive 3% strain-hardening (EPH) model represents the non-degrading and non-evolutionary SDOF system The degrading and evolutionary SDOF system (ESD) comprises a -10% strain-hardening (10% softening) and a residual strength of 0.1 F_y. The simple peak-oriented model is considered to account for the cyclic stiffness degradation while strength cyclic deterioration is not considered (Ibarra et al., 2005). All ESD systems have ductility before reaching the residual strength, evaluated as the ratio between ultimate displacement (Δ_u) and yielding displacement (Δ_y) in the backbone curve, i.e., a *ductility limit*, equal to 10. A mass-proportional viscous damping coefficient corresponding to a 5% critical damping ratio is used and kept constant throughout the time history analyses.

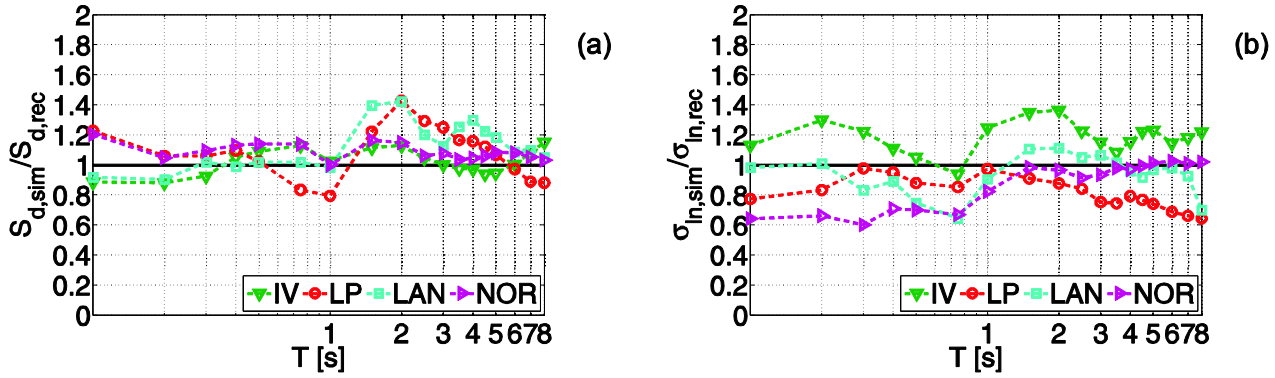

Figure 2 Ratios of the medians (a) and standard deviations (b) of the elastic displacement spectra for simulated GMs to the corresponding quantity computed for the recorded GMs.

Two representations of SDOF response, engineering demand parameters (EDP), are considered in this investigation: *inelastic displacement* ($\Delta_{inelastic}$), and *equivalent number of cycles* (N_e). These two parameters are considered to investigate both the peak displacement demand, and the cyclic seismic response; in particular, N_e is a parameter that well-captures the effects of GM potential with respect to structural response in terms of dissipated hysteretic energy.

Given the adopted constant-R approach, $\Delta_{inelastic}$ is computed, for each GM, from the dynamic response of the considered SDOF systems (characterized by given values of T and R) having specific levels of yielding strength relative to the strength required to maintain the system elastic (peak elastic base shear) as shown in Equation (1), where m is the mass of the system and S_a is the spectral acceleration corresponding to the considered GM at the same period (i.e., considering system with same mass and initial stiffness).

$$F_y = \frac{mS_a(T)}{R} \tag{1}$$

N_e is given by the cumulative hysteretic energy (E_H), evaluated as the sum of the areas of the hysteretic cycles (not considering the contribution of viscous damping) normalized with respect to the largest cycle, evaluated as the area underneath the monotonic backbone curve from the yielding displacement to the peak inelastic displacement, ($A_{plastic}$), see Equation (2).

$$N_e = \frac{E_H}{A_{plastic}} \tag{2}$$

Values of N_e close to 1 show the presence of a large plastic cycle in the non-linear response, while high values of N_e are indicative of the presence of many plastic cycles; N_e generally decreases with the period in the short period range and increases with R (Manfredi, 2001).

In addition, N_e varies largely depending on the GMs features, from values close to 1 for impulsive earthquakes to value of about 40 for long-duration earthquakes.

4. RESULTS AND DISCUSSIONS

All GMs (recorded and simulated) selected for each earthquake event are used as input for NLDA applied to all the SDOF systems considered, yielding a total of 36,000 NLDAs performed. Only horizontal component of GMs (i.e., north-south, NS, and east-west, EW) are used, while the vertical component is neglected. The spectral responses for the two horizontal components at each station are computed and then combined into an "average" spectral response by using the geometric mean. For each earthquake and each EDP ($\Delta_{inelastic}$ and N_e), the median value (i.e., the exponential of the mean of the natural log of the EDP across all the available stations) for the synthetic records divided by the median value for the real dataset is computed and plotted across the considered period range (for different R values). A ratio above unity, if statistically significant, means overestimation of response by simulations, and the opposite if smaller than one. For instance, a ratio of the medians of $\Delta_{inelastic}$ obtained using synthetics and recorded motions larger than one indicates that the synthetic records tend to produce, on average, systematically more damaging nonlinear spectral displacements than real records. Conversely, deviations below unity indicate that the simulated records tend to be, on average, more benign in producing nonlinear responses than those in nature.

In order to provide a measure of inherent intra-event variability in the simulations compared to that of real GMs, the ratio of the standard deviation (of the natural log of the data) for simulated and recorded GMs (for all sites and distances in a given earthquake) is plotted as a function of the period and R. A line above unity means relatively more record-to-record variability produced by simulated GMs whereas the opposite is true for a line below one.

A direct comparison of response statistics is acceptable as the simulated datasets are developed to match exactly the same earthquakes and site conditions (i.e. at the same stations) of the real recordings.

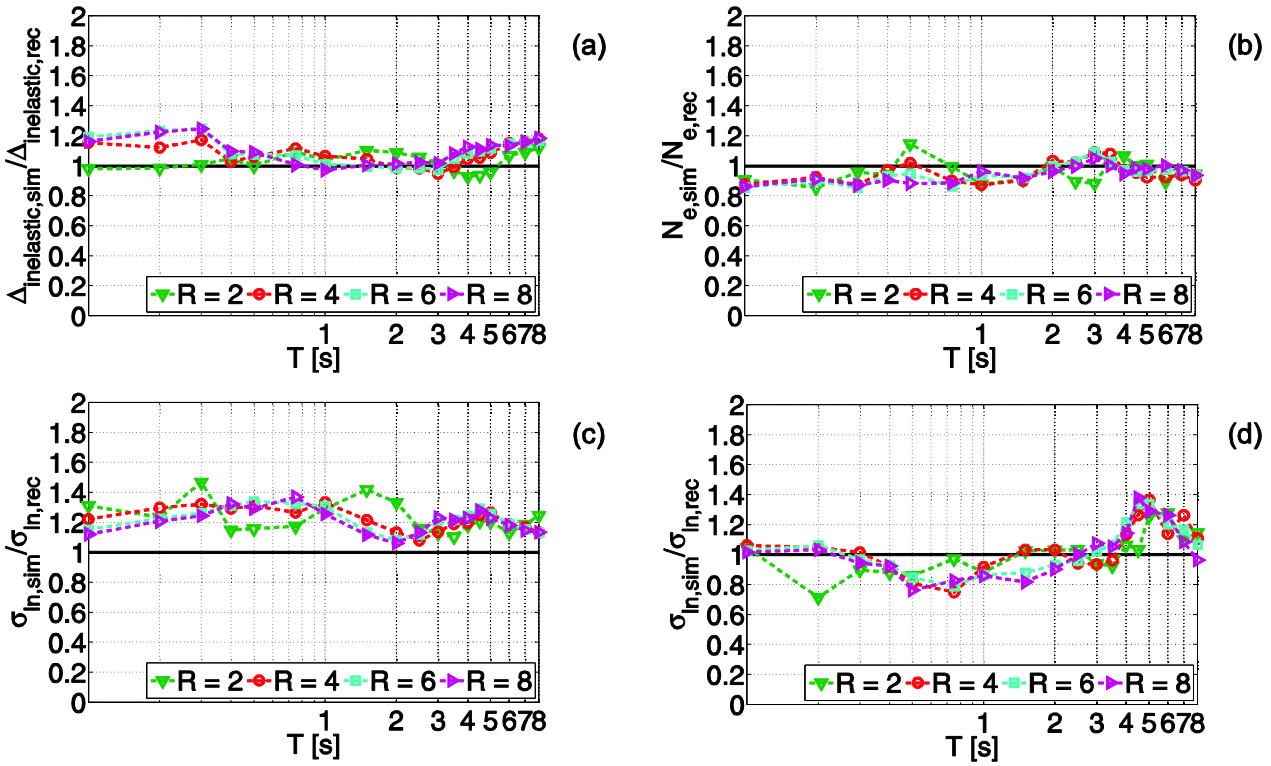

Figure 3 Ratios of the medians [(a), (b)] and standard deviations [(c), (d)] of the inelastic spectra (in terms of $\Delta_{inelastic}$ and N_e) for simulated GMs to the corresponding quantity computed for the recorded GMs for the Imperial Valley earthquake (EPH model).

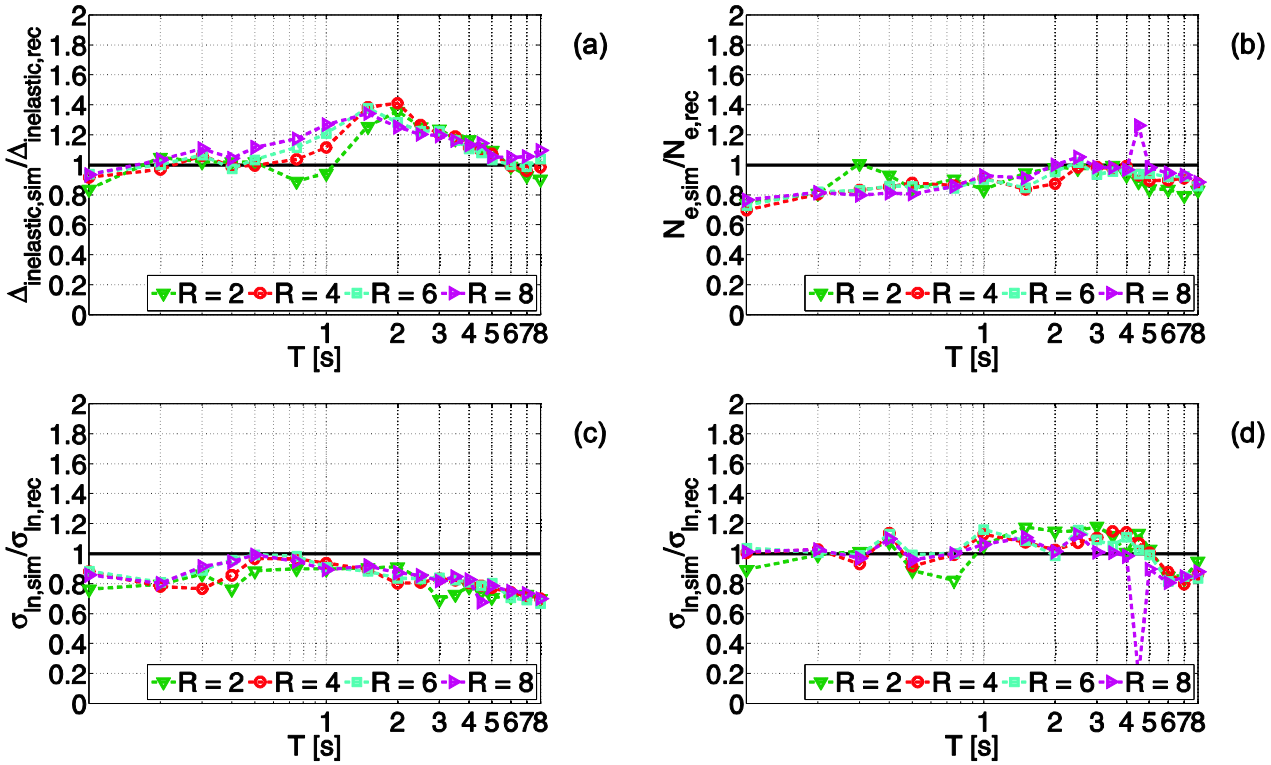

Figure 4 Ratios of the medians [(a), (b)] and standard deviations [(c), (d)] of the inelastic spectra (in terms of $\Delta_{inelastic}$ and N_e) for simulated GMs to the corresponding quantity computed for the recorded GMs for the Loma Prieta earthquake (EPH model).

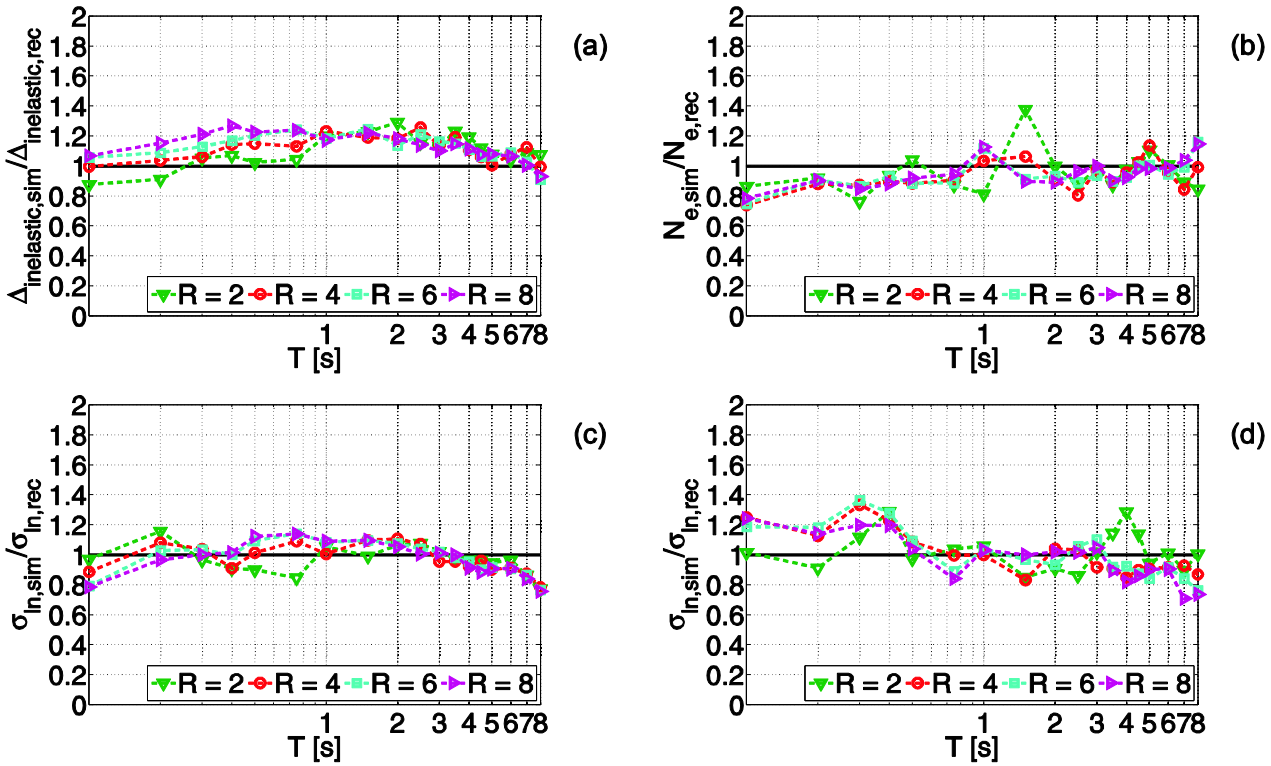

Figure 5 Ratios of the medians [(a), (b)] and standard deviations [(c), (d)] of the inelastic spectra (in terms of $\Delta_{inelastic}$ and N_e) for simulated GMs to the corresponding quantity computed for the recorded GMs for the Landers earthquake (EPH model).

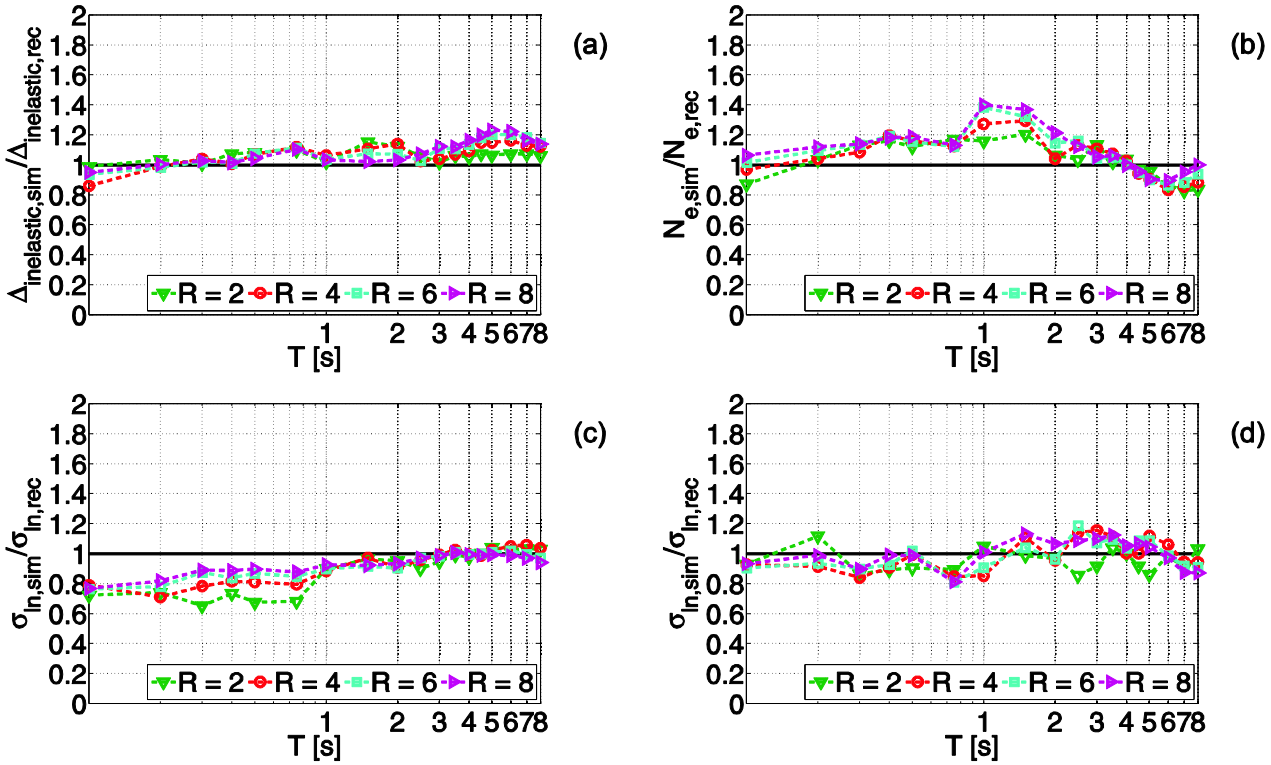

Figure 6 Ratios of the medians [(a), (b)] and standard deviations [(c), (d)] of the inelastic spectra (in terms of $\Delta_{inelastic}$ and N_e) for simulated GMs to the corresponding quantity computed for the recorded GMs for the Northridge earthquake (EPH model).

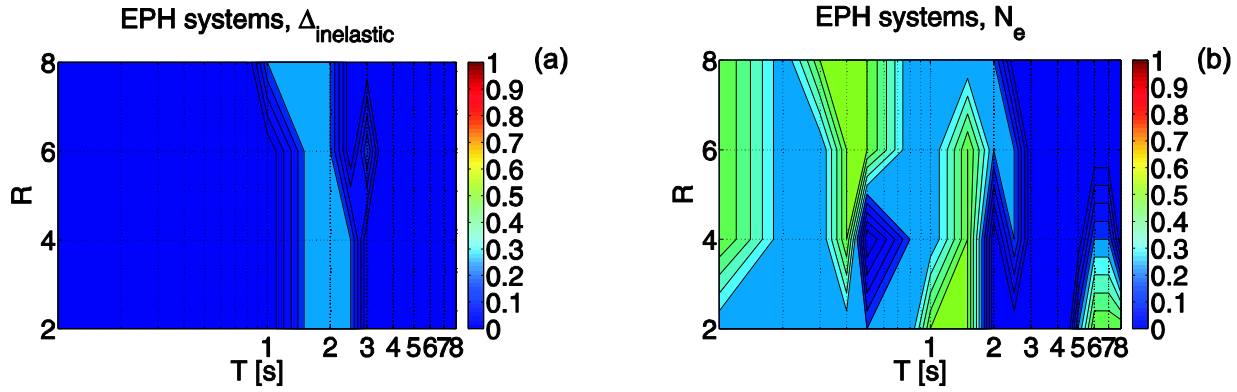

Figure 7 Percentages of hypothesis test rejections ($\alpha = 0.05$) for the EPH systems; (a) $\Delta_{inelastic}$ results and (b) N_e results.

4.1 Comparison between statistical measures of elastic response spectra

Elastic response spectra provide succinct features of peak response of linear elastic SDOF systems to strong GMs and are very often used as seismic intensity measure for a broad range of purposes. For each of the four events considered in this study, the median value of the elastic displacement spectral ordinates for the simulated records divided by the median value for the recorded dataset is computed and plotted across the considered period range in Figure 2a. In this figure, "IV" represents the Imperial Valley event with a green line and inverted triangles markers, "LP" represents Loma Prieta event with a red line and circle markers, "LAN" represents Landers event with cyan line and square marker, and "NOR" represents Northridge event with magenta line and horizontal triangle markers. In general, the elastic spectra of the simulated waveforms agree reasonably well with the observations.

In particular, in the case of the Imperial Valley and the Northridge earthquakes, the model bias (i.e., the departure of the considered ratio from unity) is near zero (< +20%) for all components across the entire bandwidth indicating that simulations are accurately reproducing the main characteristics of the observed GMs, with a slight overestimation. The comparison for the Landers event exhibits a larger model bias (about 40%) across the frequency range (1.5s-5s). Hypothesis tests (to follow) do not confirm these differences to be statistically significant. In the case of the Loma Prieta event, some differences are evident around the period of 2s; nevertheless, again, hypothesis tests (to follow) confirm these differences are not statistically significant.

From inspecting the graphs in Figure 2a, it is clear that not only the median spectral amplitudes but also shapes of the response for simulated GMs can be different than the median response spectrum from the real recordings. In fact, any trend across period in the median ratios shown in Figure 2a that departs from a horizontal line suggests that the elastic spectra generated by the synthetic model have, on average, a different shape than those produce by nature. The difference in spectral shape is large especially for Loma Prieta and Landers events, for a wide range of periods.

Except for the Imperial Valley event, the standard deviations of the spectra of the real records are generally larger compared to the simulated GMs, particularly at the shorter periods (Figure 2b). This trend of relatively low intra-event variability in the simulations has been noted previously by Star et al (2011). Seyhan et al (2012) have recently proposed a revision to the simulation approach that incorporates greater stochastic variability in the high frequency portion to address this issue, although this revision has not yet been applied to the simulations considered in the current analysis. In the case of the Imperial Valley event, the standard deviation of response of simulated records are larger than those of recorded ones across the entire period range (the considered ratio is almost constant and above the unity). This can be likely attributed to the presence in the simulated dataset of GMs featuring strong coherent velocity pulses and then large elastic response, as discussed in the following.

The differences in the elastic response between the simulated and real records have an influence on the nonlinear response statistics at all strengths levels.

4.2 Comparison between statistical measures of inelastic response spectra

Figure 3a shows the ratio of the median spectrum in terms of $\Delta_{inelastic}$ from the simulated GMs to the median spectrum (again in terms of $\Delta_{inelastic}$) from the recorded GMs for Imperial Valley and EPH model; Figure 3b shows the same ratio in terms of N_e. Figure 3c shows the ratio of the standard deviations of the data in terms of $\Delta_{inelastic}$ from the simulated GMs to the standard deviation of the data (again in terms of $\Delta_{inelastic}$) from the recorded GMs; Figure 3d shows the same ratio in terms of N_e. Figures 4-6 are developed in the same fashion as Figure 3, for the Loma Prieta, Landers and Northridge events respectively (results for the ESD model are not shown to save space; similar observations can be drawn for this case).

Looking at post-elastic response, bias in estimation of seismic response of SDOF systems depends on the considered earthquake event, period, and strength level. Results are very similar for both EPH and ESD systems, although, in the case of ESD systems the differences are slightly larger and more R dependent. Systematic deviations seem to be concentrated in the zone of semi-stochastic simulation (at very short periods), around 1s, for some cases, and at the very long periods (especially at high nonlinearity

levels). The fact that bias in terms of peak response is close to zero in the moderate-long periods part of the inelastic spectra is essentially the result of the equal displacement rule (Veletsos and Newmark, 1960), quite well observed for both recorded and simulated GMs. The observed differences at given periods are likely due to systematic differences in the average shape around those periods of the linear response spectra generated by synthetic and by real GMs. When the response of an SDOF systems becomes severely nonlinear, its effective vibration period lengthens significantly, especially at short periods, and, therefore, it becomes dependent on the frequency content of the record in a fairly large bandwidth and not only in the neighborhood of the initial elastic natural period of vibration.

As in the elastic case, simulated records tend to produce nonlinear demands that are often less variable (i.e., lower intra-event variability is observed) compared to those caused by real records, although some exceptions exist. From a practical standpoint, if an engineer seeks to design a new structure or assess the safety of an existing one against collapse, the use of simulated records that tend to generate less variable response would underestimate the likelihood of extreme response values and, therefore, the probability of collapse. The relative variability of nonlinear demands to simulated and recorded GMs is model-dependent and varies with the structural period, the level of nonlinearity, and the considered earthquake event.

4.3 Statistical significance of the difference between SDOF demands to simulated and recorded historical motions

As in Iervolino et al. (2010), parametric hypothesis tests are performed to quantitatively assess the statistical significance of the results found in terms of median response (for each oscillation period in the considered range, each R value and each nonlinear model) to recorded and simulated GMs; i.e., to asses if the ratios analyzed in the previous section differ systematically from one. Hypothesis tests are performed for both peak and cyclic EDPs, assuming a lognormal distribution for both the response parameters of interest, $\Delta_{inelastic}$ and N_e. This distribution assumptions are checked with the Shapiro-Wilk (Shapiro and Wilk, 1965) test and could not be rejected at the 95% significance level. A similar parametric hypothesis test has been performed in terms of comparison between variances for the two datasets (recorded and simulated) corresponding to each earthquake. The results, not reported here for the sake of brevity, confirm that the differences discussed in the previous sections in terms of record-to-record variability may be statistically significant, as expected by the visual inspection of Figures 3-6.

The null hypothesis is that the median EDPs for simulated GMs is equal to those from recorded GM. To this aim, a two tails Aspin-Welch (Welch, 1938) test is preferred to the standard Student t-test as the former does not require the assumption of equal, yet still unknown, variances of populations originating the samples (an unreasonable assumption given the results found in the previous section, i.e., the natures of the compared record classes). The statistical test employed is reported in Equation (3), in which z_x and z_y are the sample means, s_x and s_y are the sample standard deviations and m and n are the sample sizes (in this case always equal for each earthquake).

$$t = \frac{z_x - z_y}{\sqrt{\frac{s_x^2}{n}} + \sqrt{\frac{s_y^2}{m}}} \tag{3}$$

The test statistic, under the null hypothesis, has a Student t-distribution with the number of degrees of freedom given by Satterthwaite's approximation (Satterthwaite, 1941).

Hypothesis tests confirm that the only period range where the ratios in terms of $\Delta_{inelastic}$ significantly (assuming a 95% significance level) differ from one is approximately between 1s and 2.5s for Loma Prieta earthquake. In terms of N_e, the period ranges where the considered ratios significantly differ from one are approximately: between 0.1s and 1.5s for Loma Prieta and EPH model; between 0.3s and 2.5s for Northridge and EPH model and 0.1 and 3s for Northridge and ESD model. In the other cases, the rejections are sparse and randomly distributed in the whole periods range.

In order to summarize the hypothesis tests results and draw conclusions, percentage of hypothesis tests rejections (assuming a 95% significance level) are shown in Figures 7 for each pair (T, R), for EPH system and for $\Delta_{inelastic}$ and N_e,, respectively. In computing these percentages, all the earthquakes are considered together. Based on these figures, tests have shown a statistical significance of the bias of simulated records in terms of inelastic displacement only at very short periods and between 1s and 2.5s, for all the considered nonlinearity levels. The differences in this latter periods range are likely due to the large differences in both absolute and relative amplitudes (i.e., the shape) of elastic response for Loma Prieta and Landers events. In terms of equivalent number of cycles, the differences found have statistical significance in the short periods range (< 2s), especially in the case of ESD systems (not shown here), with some other sparse rejection for very long periods. In general, these results confirm the considerations based on the visual inspection of Figures 3-6. In some cases, the limited sample size and the relatively large variability prevent us from stating that the median inelastic spectra (in terms of both $\Delta_{inelastic}$ and N_e) generated by simulated GMs are systematically different than those produced by recorded GMs at the two customary significance levels (i.e., 5% and 10%).

4.4 Effect of I_D

Empirical observations and analytical studies show how cyclic structural damage is related to energy released during ground shaking, and then, to the duration of GM.

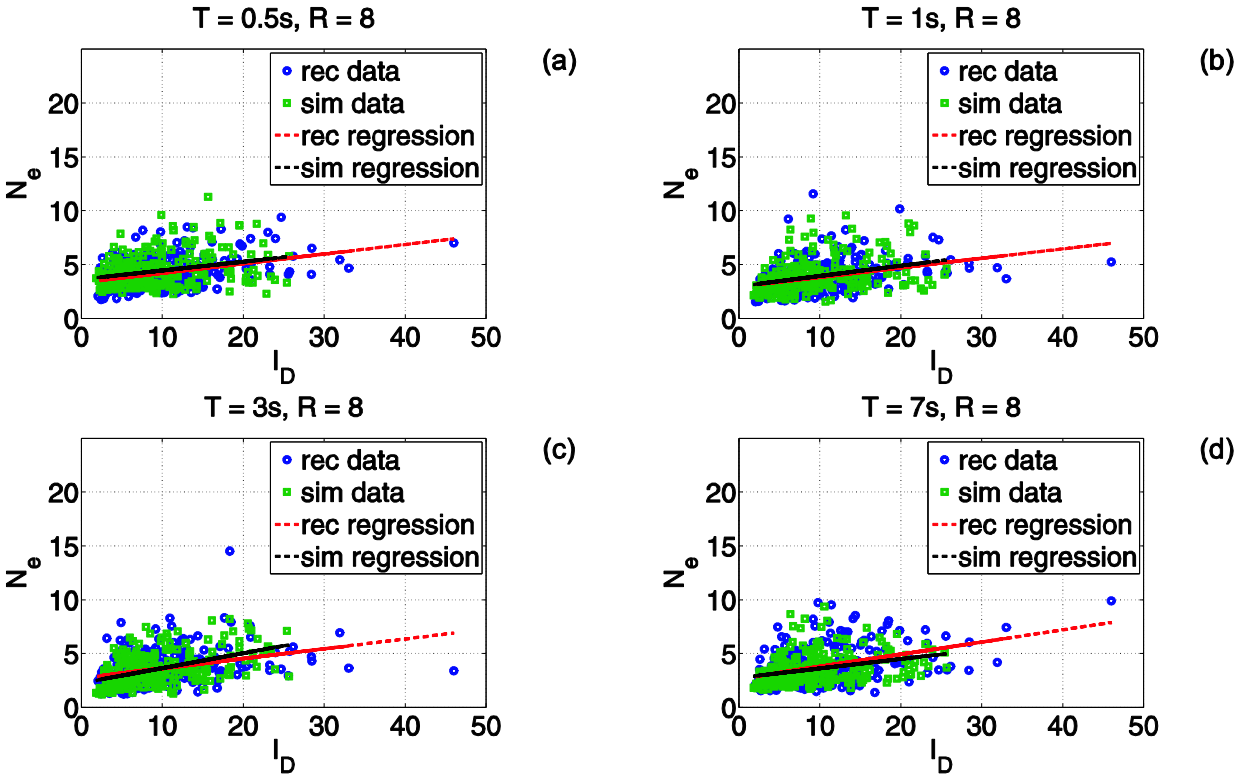

Figure 8 N_e versus I_D ratio for R = 8 and different T values (ESD systems).

Table 1 Average values of I_D for the considered datasets

	Simulated	Recorded
Imperial Valley	6.8	7.8
Loma Prieta	7.1	8.6
Landers	12.9	16.2
Northridge	11.2	9.7

Table 2 Number of FN GMs identified as pulse-like using the classification procedure proposed by Baker (2007)

	Simulated	Recorded	Both
Imperial Valley	12	14	12
Northridge	5	6	3

Each accelerograms has been processed to evaluate its characteristics in terms of the so-called *Cosenza and Manfredi index* (I_D) (Manfredi, 2001). This dimensionless index I_D has proven to be a good proxy for cyclic structural response (Iervolino et al., 2006); it is defined in Equation (4) where $a(t)$ is the acceleration time-history, t_E is the total duration of the seismic event, and PGA and PGV are the peak ground acceleration and velocity respectively.

$$I_D = \frac{\int_0^{t_E} a^2(t)\,dt}{\mathrm{PGA}\cdot\mathrm{PGV}} \qquad (4)$$

In Figure 8, the N_e values for recorded and simulated datasets are plotted as a function of I_D for four selected periods (0.5s, 1s, 3s, and 7s) and for R = 8; all the earthquakes are considered together in the panels of Figure 8. For the sake of brevity and based on the findings of the previous sections, only results for ESD systems are presented (result for EPH systems are substantially equivalent). The estimated linear regressions (dotted red and black lines for recorded and simulated GMs respectively) are also reported in Figure 8.

Figure 8 reveals that both the level and trend of the observed values (i.e. N_e to recorded GMs) as a function of I_D are matched well by the simulation. Moreover, it is possible to note a fairly good correlation between the two parameters, confirming that differences in cyclic response are predictable looking at the integral (duration-related) intensity measures, characterizing each record (e.g., Iervolino et al, 2006).

Table 1 reports average values of I_D for each dataset. These values summarize to explain the differences found in terms of general underestimation (Imperial Valley, Loma Prieta and Landers) and overestimation (Northridge) by simulation, in terms of N_e.

4.5 Presence of pulse-like records.

In the case of an earthquake, ground motion recorded at near-source sites may be subjected to rupture directivity effects which result in a low frequency full cycle velocity pulse at the beginning of the signal. The occurrence of this effect depends on the rupture process, on the geometrical configuration of the fault and the site and other factors, Somerville et al., 1997.

Elastic demand amplitude of pulse-like signals is generally larger than that of ordinary recordings, particularly concerning the fault-normal (FN) direction; also the spectral shape is non-standard with an increment of spectral ordinates in the range around the pulse period (Chioccarelli and Iervolino, 2010).

NGA records, were classified as *pulse-like* and *non-pulse-like* by Baker (2007) via a wavelets-based algorithm, which assigns a score, a real number between 0 and 1, to each record and determines the pulse period (T_p). The larger the score the more likely the record is to show a pulse. Only the FN ground motions having a pulse score equal to or larger than 0.85 were, arbitrarily, counted as pulse-type records. In particular, according to Baker's study, Imperial Valley and Northridge events present several GMs classified as pulse-like, i.e., 15 and 11 respectively, while Loma Prieta and Landers feature only 4 and 3 pulse-like GMs.

In this section, the algorithm proposed by Baker is applied to the recorded and simulated datasets for Imperial Valley and Northridge events in order to investigate possible differences in terms of pulse-like GMs and then possible sources of the differences found in the previous sections in terms of structural response. For each earthquake and each dataset, horizontal components have been rotated into fault-parallel (122° azimuth for Northridge, 143° azimuth for Imperial Valey) and fault-normal (212° azimuth for Northridge, 233° azimuth for Imperial Valley) orientations.

Table 2 reports, for each earthquake, the number of identified pulse-like records in the recorded dataset (this number is slightly different from that reported in Baker because here only a subset of NGA stations has been considered for each event), in the simulated dataset and the number of records classified as pulse-like in both datasets. Table 2 shows that simulations for Imperial Valley reproduce well the number of pulse-like GMs in the recorded dataset (12/14) while for Northridge only 3/6 GMs are classified as pulse-like in both datasets (two additional GMs are identified as pulse-like in the simulated dataset and not in the NGA). Analysis shows that some significant differences exist in the values of T_p even for the GMs classified as pulse-like in both datasets: in the case of Imperial Valley, T_p values for the recoded dataset are, on average, 25% larger than T_p values in the simulated dataset; for Northridge T_p values for the simulated dataset are, on average, 31% larger than T_p values in the recorded dataset (but this percentage is computed on only 3 GMs). These discrepancies can likely explain the differences found in comparing structural response and its variability to simulated and recorded GMs at least for these two events. In particular, in the case of Imperial Valley, the simulations likely tend to produce stronger directivity effects on ground motion amplitudes than they should (because of too strong coherence in the rupture descriptions) with large variance. Generally, it is difficult to quantify/calibrate this since directivity effects seem to be underestimated by current empirical models due to the scarcity of recordings. The pulse-period classification of Baker (2007) gets at part of this issue, but it does not really address the amplification due to directivity.

It is evident that strong directivity effects in the simulations require more study. This is needed for validation, and the simulations may also help refine directivity prediction models.

5. CONCLUSIONS

In this study, simulated and recorded GMs were compared in terms of elastic and post-elastic seismic peak and cyclic response. This was pursued by considering SDOF systems with two different force-displacement backbones and hysteretic rules at different nonlinearity levels and for several fundamental periods. The inelastic displacement ratio and the equivalent number of cycles response of 144 systems were analyzed with respect to recorded and simulated GMs for four historical earthquakes: 1979 M_w = 6.5 Imperial Valley, 1989 M_w = 6.8 Loma Prieta, 1992 M_w = 7.2 Landers, and 1994 M_w = 6.7 Northridge.

Results of this study show, in the context of the SDOF systems used, that simulation matches well the median peak seismic demands produced by recorded GMs and that observed differences are generally not statistically significant across the entire frequency bandwidth. However, for certain structural systems, simulated accelerograms may produce median inelastic demand different from a similar estimate using corresponding recorded motions. In particular, the simulation appears to be biased especially in the transition area between semistochastic and deterministic simulation for the Loma Prieta event (around 1s). The observed differences are due to systematic differences in the average shape around those periods of the linear response spectra generated by synthetic and by real GMs.

Also in terms of cyclic response some differences are observed, again mostly in the short periods range where the simulation is semistochastic. The discrepancies found in terms of median demands and their variability depend on the considered earthquake, the structural period, the non-linearity level and the hysteretic model used, although without any clearly systematic trends. However, it worth nothing that, as well known, the cyclic response differences could be predicted by some integral parameters of GM.

Some differences exist in the number of pulse-like GMs in the simulated dataset (with respect to the recorded one for the same earthquake) and in the values of pulse periods for these records, confirming that strong directivity effects in the simulations require more study.

The results of this study are directly relevant to the engineering community establishing validated reference sets

of synthetically generated broadband GM, and they may also provide feedback for seismologists who generate simulated GMs for engineering applications.

Acknowledgements:
This research was supported by *Rete dei Laboratori Universitari di Ingegneria Sismica* – ReLUIS for the research program founded by the Italian Department of Civil Protection – Executive Project 2010-2013, and the NSF sponsored Southern California Earthquake Center (SCEC). Their support is gratefully acknowledged. Any opinions, findings, and conclusions or recommendations expressed in this paper are those of the authors and do not necessarily reflect the views of the sponsors. The first author also acknowledges the travel grant provided by Tokyo Institute of Technology, Japan.

References:

Baker, J.W. (2007), "Quantitative classification of near-fault ground motions using wavelet analysis," *Bulletin of the Seismological Society of America*, **97**(5), 1486-1501.

Bazzurro, P., Sjoberg, B., and Luco, N. (2004a), "Post-elastic response of structures to synthetic ground motion," Report for Pacific Earthquake Engineering Research (PEER) Center Lifelines Program Project 1G00 Addenda.

Bazzurro, P., Sjoberg, B., Luco, N., Silva, W., and Darragh, R. (2004b), "Effects of Strong Motion Processing Procedures on Time Histories, Elastic and Inelastic Spectra," *Proc. Invited Workshop on Strong-Motion Record Processing*, Convened by COSMOS, Richmond, CA, May 26-27.

Campbell, K.W. and Bozorgnia, Y. (2008), "NGA ground motion model for the geometric mean horizontal component of PGA, PGV, PGD and 5% damped linear elastic response spectra for periods ranging from 0.01 to 10 s," *Earthquake Spectra*, **24**, 139–171.

Chioccarelli, E., and Iervolino, I. (2010), "Near-Source Seismic Demand and Pulse-Like Records: a Discussion for L'Aquila Earthquake," *Earthquake Engineering and Structural Dynamics*, **39**(9), 1039–1062.

Graves, R.W., and Pitarka, A. (2010), "Broadband Ground-Motion Simulation Using a Hybrid Approach," *Bulletin of the Seismological Society of America*, **100**(5A), 2095-2123.

Graves, R.W., and Aagaard, B.T. (2011), "Testing long-period ground-motion simulations of scenario earthquakes using the M w 7.2 El Mayor-Cucapah mainshock; evaluation of finite-fault rupture characterization and 3D seismic velocity models," *Bulletin of the Seismological Society of America*, **101**(2), 895-907.

Haselton, C.B., Editor (2009). "Evaluation of Ground Motion Selection and Modification Methods: Predicting Median Interstory Drift Response of Buildings," PEER Report 2009/01, Pacific Engineering Research Center, University of California, Berkeley, California.

Ibarra, L.F., Medina, R.A., and Krawinkler, H. (2005), "Hysteretic Models that Incorporate Strength and Stiffness Deterioration," *Earthquake Engineering and Structural Dynamics*, 34, 1489-1511.

Iervolino, I., De Luca, F., and Cosenza E. (2010), "Spectral shape-based assessment of SDOF nonlinear response to real, adjusted and artificial accelerograms," *Engineering Structures*, 32(9), 2776-279.

Iervolino, I., Manfredi, G., and Cosenza, E. (2006), "Ground-motion duration effects on nonlinear seismic response," *Earthquake Engineering and Structural Dynamics*, **35**, 21-38.

Manfredi, G. (2001), "Evaluation of seismic energy demand," *Earthquake Engineering and Structural Dynamics*, 30, 485-499.

Naeim, F., and Graves, R.W. (2006), "The case for seismic superiority of well-engineered tall buildings," *The Structural Design of Tall and Special Buildings*, **14**(5), 401–416.

Olsen, K.B., Day, S.M., and Bradley, C.R. (2003), "Estimation of Q for long-period (>2 s) waves in the Los Angeles Basin," *Bulletin of the Seismological Society of America*, **93**, 627-638.

Satterthwaite, F E. (1941), "Synthesis of variance," *Psychometrika*, **6**, 309-316.

Seyhan, E, Stewart, J.P. and Graves, R.W. (2012), "Calibration of a Semi Stochastic Procedure for Simulating High Frequency Ground Motions," *Earthquake Spectra* (*sumbitted*).

Shapiro, S.S., and Wilk, M.B. (1965), "An analysis of variance test for normality (complete samples)," *Biometrika*, **52**, 591-611.

Star, L., Stewart, J.P., and Graves, R.W. (2011), "Comparison of Ground Motions from Hybrid Simulations to NGA Prediction Equations," *Earthquake Spectra*, **27**, 331-350.

Somerville, P. G. (1993), "Engineering applications of strong ground motion simulation," *Tectonophysics*, **218**(1-3), 195-219.

Somerville, P. G., Smith N. F., Graves, R. W., and Abrahamson, N. A. (1997), "Modification of Empirical Strong Ground Motion Attenuation Relations to Include the Amplitude and Duration Effects of Rupture Directivity," *Seismological Research Letters*, **68**, 199-222.

Veletsos, A. S., and Newmark, N. M. (1960), "Effect of inelastic behavior on the response of simple systems to earthquake motions," *Proc. of 2nd World Conference on Earthquake Engineering*, Vol. 2, 895–912.

Welch, BL. (1938), "The significance of the difference between two means when the population variances are unequal," *Biometrika*, **29**, 350-362.